DOI: 10.1002/chem.200801685

$[M(N_3)_2(H_2O)_2]\cdot$(bpeado): Unusual Antiferromagnetic Heisenberg Chain (M = Mn) and Ferromagnetic Ising Chain (M = Co) with Large Coercivity and Magnetic Relaxation (bpeado = 1,2-Bis(4-pyridyl)ethane-*N*,*N*′-dioxide)

Hao-Ling Sun,[a, b] Zhe-Ming Wang,*[a] and Song Gao*[a]

Abstract: We present here the structures and magnetism of two isostructural magnetic metal-azido chain compounds of the type $[M(N_3)_2(H_2O)_2]\cdot$(bpeado) (**1**, M = Mn; **2**, M = Co; bpeado = 1,2-bis(4-pyridyl)ethane-*N*,*N*′-dioxide), prepared by utilizing the long spacer bpeado. The structure is composed of $[M(N_3)_2(H_2O)_2]_n$ metal-azido chains, in which metal ions are bridged by two end-on azido ligands, and the chains are further supported by H-bonding interactions between the coordination water of the chain and the lattice bpeado in a three-dimensional (3D) threefold interpenetrated H-bonded framework. Within the structure, the metal-azido chains are separated quite well. Investigation of the magnetic properties has revealed that the Mn compound **1** is an isotropic Heisenberg chain with unusual antiferromagnetic coupling between the Mn^{2+} ions linked by double end-on azide anions. The Co compound **2** shows a strong anisotropic Ising-type ferromagnetic chain within the material. Detailed magnetic studies on both polycrystalline and single-crystal samples of **2** have revealed a large coercivity of up to 37.5 kOe (along the crystallographic *b*-axis), multi-magnetic transitions, and single-chain-magnet-like magnetic relaxation behavior.

Keywords: azides · Heisenberg chain · Ising chain · magnetic properties · single-chain magnets

Introduction

Magnetic chain compounds have attracted continuous interest because they provide genuine opportunities to explore the fundamental aspects of magnetic interactions and magneto-structural correlations in molecular systems.[1] Recently, magnetic chain compounds with large uniaxial anisotropy have been extensively investigated because these Ising anisotropic chains offer the possibility of studying single-chain magnets (SCMs) with unique physical properties.[2–8] For synthetic chemists, the approach for building such chain compounds is to utilize appropriate bridging ligands as effective magnetic couplers to link the spin carriers into one-dimensional (1D) chains, in conjunction with specific spacers to separate these chains.[3–8] The magnetic anisotropy of the spin carriers is another key factor that affects the magnetic behavior of such 1D systems.[1] If isotropic ions are employed, isotropic Heisenberg chains are to be expected, whereas if anisotropic metal ions are used, Ising chains and hence SCMs can be expected. Short ligands, such as hydroxyl,[4] cyano,[5] azido,[6] oxalato/oxamate,[7] and carboxylate,[8] have most commonly been employed as bridging ligands because they can efficiently transmit magnetic coupling. Among these ligands, azide is extremely popular due to its versatile bridging modes, which facilitate the assembly of coordination complexes with different topologies and magnetic properties.[6,9–11] The azido ion is capable of linking two or more metal centers in various modes, such as μ-1,1 (end-on, EO), μ-1,3 (end-to-end, EE), μ-1,1,3, and others, giving rise to a variety of multidimensional coordination polymers.[9,10] The two main coordination modes, EO and EE, can serve as good mediators for transmitting ferromagnetic (FO) interactions (mainly EO) or antiferromagnetic (AF) interactions (mainly EE). The combination of ancillary multidentate ligands, such as pyridine derivatives or organic amides, with metal-azide systems has provided a wealth of magnetic

[a] Dr. H.-L. Sun, Prof. Dr. Z.-M. Wang, Prof. Dr. S. Gao
Beijing National Laboratory for Molecular Sciences
State Key Laboratory of Rare Earth Materials Chemistry and Applications
College of Chemistry and Molecular Engineering
Peking University, Beijing 100871 (PR China)
Fax: (+86) 10-6275-1708
E-mail: zmw@pku.edu.cn
gaosong@pku.edu.cn

[b] Dr. H.-L. Sun
Department of Chemistry, Beijing Normal University
Beijing 100875 (PR China)

Supporting information for this article is available on the WWW under http://dx.doi.org/10.1002/chem.200801685.

 © 2009 Wiley-VCH Verlag GmbH & Co. KGaA, Weinheim WILEY InterScience DISCOVER SOMETHING GREAT

chain compounds, including FO chains with double-EO azide,[6a,9] AF chains with single- or double-EE azide,[6b] and, in particular, topologically ferrimagnetic (FI) EO/EE/EE and EO/EO/EO/EO/EE alternating chains.[10] Among them, only a few SCMs or SCM-like compounds have been successfully constructed by employing anisotropic metal ions, such as Co^{2+},[6a] Ni^{2+},[6b] and Mn^{3+}.[6c] Many magnetic chain compounds have been constructed by utilizing bulky co-ligands or bulky counter ions to weaken the interchain interaction.[3,6,8b,11] In this work, however, we have set out to explore whether long ditopic ligands can be used as spacers to effectively separate magnetic chains. In this context, 1,2-bis(4-pyridyl)ethane-*N*,*N*′-dioxide (abbreviated hereafter as bpeado) is a good choice because it is a tried-and-tested long spacer for separating metal centers, having been quite widely used in the construction of metal–organic frameworks.[12] On the other hand, weakly-coupled SCM compounds have attracted great attention recently because they have proved capable of exhibiting fantastic magnetic behavior, such as very large coercivity, multiple magnetic transitions, and so on,[13] parallel to the study of weakly-coupled single-molecular magnet (SMM) compounds.[14] Here, we report two new magnetic chain compounds of the type $[M(N_3)_2(H_2O)_2]\cdot$(bpeado) (**1**, M = Mn; **2**, M = Co), constructed by using azide as a bridging and coupling ligand and bpeado as a spacer. The two compounds consist of double-EO-azido-bridged chains of $[M(N_3)_2(H_2O)_2]_n$ weakly linked by bpeado through H-bonds in a threefold interpenetrated 3D H-bonding framework. Compound **1** is an unusual AF-coupled Heisenberg chain. Compound **2** is a strong Ising-type FO chain, with a rather large coercivity of 37.5 kOe along the crystallographic *b* axis and SCM-like behavior, as has been established by magnetic investigations of both polycrystalline and single-crystal samples.

Results and Discussion

Crystal structures: Single-crystal X-ray structure determinations and powder X-ray diffraction (PXRD) analyses (see the Experimental Section and Figure S1 in the Supporting Information) revealed compounds **1** and **2** to be isomorphous, crystallizing in the orthorhombic space group *Pccn* (Table 1). The structure is composed of a homometallic chain of $[M(N_3)_2(H_2O)_2]_n$ supported by lattice bpeado molecules through H-bonding (Figure 1). Within the $[M(N_3)_2(H_2O)_2]_n$ chain (Figure 1, top), the adjacent M^{2+} ions are bridged by two EO-azido ligands. The unique M^{2+} ion, located at the twofold axis (1/4, 3/4, *z*; Wyckoff position 4*d*), is surrounded by four equatorial nitrogen atoms from four EO-azido bridges (Mn/Co-N = 2.252/2.175 Å) and two axial water molecules (Mn/Co-O = 2.157/2.070 Å) (Table 2). These form a slightly compressed MN_4O_2 octahedron with its axial direction O-M-O along the crystallographic *a* axis and the MN_4 base plane nearly parallel to the *bc* plane (Figure 1, top). The *cis* N/O-M-N/O angles are 78.5 to 101.6°, while the *trans* angles are 174.8 to 179.9° (Table 2).

Table 1. Crystal data and structure refinement for **1** and **2**.

Compound	**1**	**2**
formula	$C_{12}H_{16}MnN_8O_4$	$C_{12}H_{16}CoN_8O_4$
F_w	391.27	395.26
crystal system	orthorhombic	orthorhombic
space group	*Pccn*	*Pccn*
a [Å]	10.3559(2)	10.2907(2)
b [Å]	22.7233(6)	22.7057(5)
c [Å]	6.8999(1)	6.7321(1)
V [Å^3]	1623.69(6)	1573.01(5)
Z	4	4
ρ_{calcd} [g cm^{-3}]	1.601	1.669
μ ($Mo_{K\alpha}$) [mm^{-1}]	0.851	1.130
crystal size [mm^3]	0.25 × 0.10 × 0.06	0.36 × 0.26 × 0.06
T_{max} and T_{min}	0.955, 0.868	0.936, 0.840
θ_{min}, θ_{max} [°]	3.59, 27.50	3.59, 27.49
F(000)	804	812
data collected	26502	22911
unique data	1860	1803
observed data [$I > 2\sigma(I)$]	1266	1318
R_{int}	0.0599	0.0539
Number of parameters	121	122
$R1$[a] [$I > 2\sigma(I)$]	0.0288	0.0287
$wR2$[b] [$I > 2\sigma(I)$]	0.0761	0.0762
$R1$[a] [all data]	0.0514	0.0459
$wR2$[b] [all data]	0.0804	0.0816
GOF	1.025	1.061
$\Delta\rho$[c] [e Å^{-3}]	+0.653, −0.298	+1.066, −0.356
Δ/σ[d], max., mean	0.001, 0.000	0.000, 0.000

[a] $R1 = \Sigma||F_o| - |F_c||/\Sigma|F_o|$. [b] $wR2 = [\Sigma w(F_o^2 - F_c^2)^2]/\Sigma w(F_o^2)^2]^{1/2}$. [c] Maximum and minimum residual electron density. [d] Maximum and mean sigma/shift.

Table 2. Selected bond lengths [Å] and angles [°] for **1** and **2**.

	1, M = Mn	**2**, M = Co
M–O1	2.157(1)	2.070(1)
M–N1	2.252(1)	2.175(2)
O1-M-O1[a]	179.55(7)	179.88(8)
O1-M-N1	87.85(5)	88.15(5)
O1-M-N1[a]	92.49(5)	91.75(6)
O1-M-N1[b]	92.74(5)	92.50(6)
O1-M-N1[c]	86.91(5)	87.60(5)
N1-M-N1[a]	80.20(7)	78.54(8)
N1-M-N1[b]	100.11(6)	101.60(7)
N1-M-N1[c]	174.76(7)	175.75(8)
N1[b]-M-N1[c]	80.06(7)	78.58(8)
M-N1-M[d]	99.87(6)	101.44(6)

Symmetry codes: [a] $-x+1/2$, $-y+3/2$, z. [b] $-x+1/2$, y, $z+1/2$. [c] x, $-y+3/2$, $z+1/2$. [d] x, $-y+3/2$, $z-1/2$.

The chain runs along the *c* direction with the unique M···M distances being 3.450 Å (Mn)/3.366 Å (Co) and the M-N_{azido}-M bridging angles being 99.9° (Mn)/101.4° (Co). The M···M distances in both compounds are similar to those in related compounds with double-EO-azido bridges between metal sites.[6a,9] The $[M(N_3)_2(H_2O)_2]_n$ chain is straight, in contrast to the helical $[Co(bt)(N_3)_2]$ chain (bt = 2,2′-bithiazoline).[6a] The chains are further connected by H-bonding between the axially coordinated water and the *N*-oxide groups of lattice bpeado molecules, with H-bonds of $O_{water}\cdots O_{bpeado} = 2.681$ to 2.694 Å, O_{water}-H···O_{bpeado} = 159.9 to 169.5°, resulting in a 3D H-bonding network (Figure 1, bottom). In fact, each *N*-

 © 2009 Wiley-VCH Verlag GmbH & Co. KGaA, Weinheim

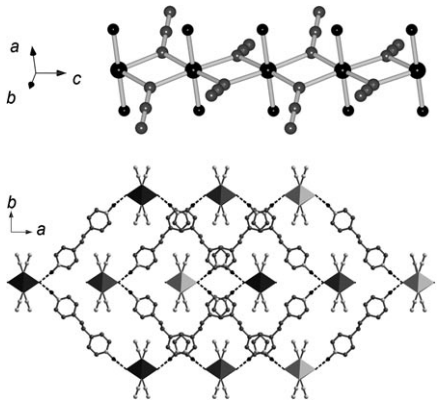

Figure 1. Structures of **1** and **2**. Top) The 1D chain of $[M(N_3)_2(H_2O)_2]_n$. Atomic scheme: M large black spheres, N grey spheres, O small black spheres. Bottom) The 3D 3-fold interpenetrated H-bonding networks viewed down the $[M(N_3)_2(H_2O)_2]_n$ chain direction. The individual nets are represented by metal polyhedra of dark, medium, and light greys. C in grey, N white, and O black, and the O_{water}-H···O_{bpeado} H-bonding in black dashed bonds. H atoms have been omitted.

oxide group of bpeado forms two nearly equal H-bonds to two water molecules of one $[M(N_3)_2(H_2O)_2]_n$ chain as a bifurcated acceptor.[15] The unique network possesses large rhombic channels along the *c* direction and open windows on the channel walls. This allows the occurrence of threefold interpenetration, with the channels of one network being threaded by the $[M(N_3)_2(H_2O)_2]_n$ chains of a further two networks, and the channel side windows being threaded by bpeado molecules (Figure 1, bottom). It may also be noted that the pyridine rings of adjacent bpeado molecules are face-to-face overlapped, with plane-to-plane separations of 3.45 Å (Mn)/3.37 Å (Co), indicating π–π interactions.[16] In spite of the interpenetration, the interchain M···M separations are longer than 10.4 Å. Therefore, the chains are quite well separated by employing the long bpeado spacers.

Magnetic properties: The magnetic properties of **1** and **2** are very different owing to the different spin carriers, isotropic Mn^{2+} in **1** and anisotropic Co^{2+} in **2**. The $\chi_M T$ value of **1** at 300 K was measured as 4.41 $cm^3 mol^{-1} K$, as expected for one isolated Mn^{2+} ion (4.375 $cm^3 mol^{-1} K$ for $S=5/2$, assuming $g=2.00$).[1a,17] It showed a continuous steady decrease upon lowering the temperature, falling to 0.80 $cm^3 mol^{-1} K$ at 2 K (Figure 2). This corresponds to the AF interaction between Mn^{2+} ions mediated by the double EO-azido bridges. The magnetic data obeyed the Curie–Weiss law with $C=$ 4.51 $cm^3 mol^{-1} K$ and $\theta=-5.6$ K (Figure S2 of the Supporting Information). The magnetic data over the whole temperature range could be well fitted by a Fisher 1D Heisenberg chain model ($S=5/2$, $H=-2JS_iS_j$),[18] resulting in $J=$ $-0.26(1)$ cm^{-1}, $g=2.02(2)$, and $R=1.8\times10^{-4}$ (R is defined as $\Sigma[(\chi_M)_{obs}-(\chi_M)_{calcd}]^2/\Sigma[(\chi_M)_{obs}]^2$). At 1.9 K, the isothermal magnetization (Figure 2, inset) increased linearly with the applied magnetic field and reached a value of 3.8 Nβ at 50 kOe; the observed magnetization was always below the Brillouin magnetization curve[1a] for uncoupled $S=5/2$ spins.

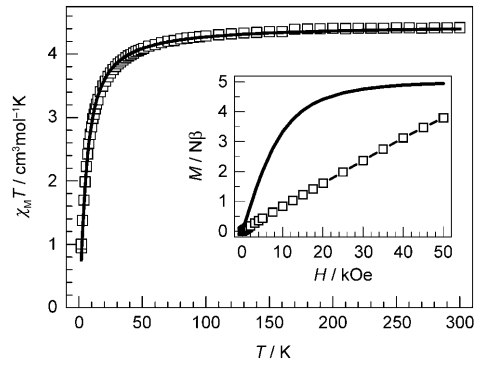

Figure 2. Magnetism of **1**. Plot of $\chi_M T$ vs T under a 100 Oe field. The black line shows the best fit obtained by using a 1D Fisher model. Inset: the isothermal magnetization at 1.9 K, with the Brillouin magnetization curve (black line) for uncoupled $S=5/2$ spins.

This confirmed the existence of AF coupling between the Mn^{2+} ions. These results clearly indicated the occurrence of rarely observed AF coupling between the double-EO-azido-bridged Mn^{2+} ions. To the best of our knowledge, this is in fact the first observation of an AF coupled Mn^{2+} chain compound with double EO-azido bridges, though it is well established that EO-azido bridges can usually mediate FO coupling.[9] The probable reason for this unusual magnetic behavior may be that the Mn-N_{azido}-Mn bridging angle of 99.9° is smaller than that found in reported EO-azido-bridged Mn^{2+} chain compounds[9] and close to the calculated angle (98°) for Mn^{2+} dimer, which favors an AF coupling pathway.[19]

One feature essential for SCM behavior is the existence of uniaxial anisotropy of the chain, which is ideally of an Ising type. Enlightened by the structural and magnetic study of **1** and the successful preparation of a Co^{2+}-azide SCM,[6a] we synthesized **2** by using anisotropic Co^{2+}, anticipating an Ising chain and SCM behavior. Indeed, **2** displayed very different magnetism to that of **1**, and its magnetic properties were investigated using both polycrystalline samples and single crystals.

The temperature dependence of the magnetic susceptibility of a polycrystalline sample of **2** under a 100 Oe field is shown in Figure 3. The $\chi_M T$ value at 300 K was measured as

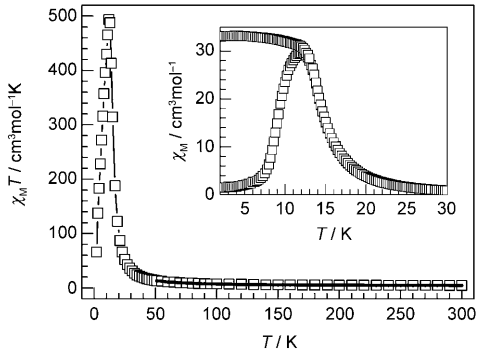

Figure 3. Magnetism of a polycrystalline sample of **2**. Plot of $\chi_M T$ *vs* T under a 100 Oe field. The black line shows the best fit obtained by using a 1D Fisher model. Inset: ZFC/FC plots under a 10 Oe field.

 © 2009 Wiley-VCH Verlag GmbH & Co. KGaA, Weinheim

4.38 $cm^3 mol^{-1} K$, which is much higher than the spin-only value of 1.88 $cm^3 mol^{-1} K$ for one spin with $S=3/2$, $g=2.00$,[1a] owing to the significant orbital contribution of the Co^{2+} ion in an octahedral environment.[1c,20] Upon cooling, $\chi_M T$ increased continuously in the high temperature range and then increased much more sharply below 50 K, reaching a maximum of 493.7 $cm^3 mol^{-1} K$ at 12.0 K, before decreasing to 91.4 $cm^3 mol^{-1} K$ on further cooling to 2 K. The magnetic susceptibility in the range 100–300 K obeyed the Curie–Weiss law with $C=4.05$ $cm^3 mol^{-1} K$ and $\theta=+45.9$ K (Figure S2 in the Supporting Information). These findings were suggestive of FO coupling between the Co^{2+} ions bridged by double EO-azido ligands within the chain. The zero-field-cooled magnetization (ZFC) and field-cooled magnetization (FC) data at a low field of 10 Oe (Figure 3, inset) displayed irreversibility below 14 K, indicating the occurrence of long-range ordering (LRO) within the material, and the critical temperature, T_C, was determined as 13.8 K from the position of the negative peak in a plot of $d\chi_M/dT$ from the FC data (Figure S3 in the Supporting Information). AC susceptibility plots (Figure 4) showed significantly high, broad, and frequency-dependent peaks in the range 11–15 K, and a further small peak below 10 K for low-frequency out-of-phase data at 111 Hz, indicating the LRO and a possible second magnetic transition in the low-temperature region. Similar AC behavior has been found for several magnetic Co chain compounds.[4,13b,c] The frequency dependence of the peaks and the second magnetic transition will be discussed later.

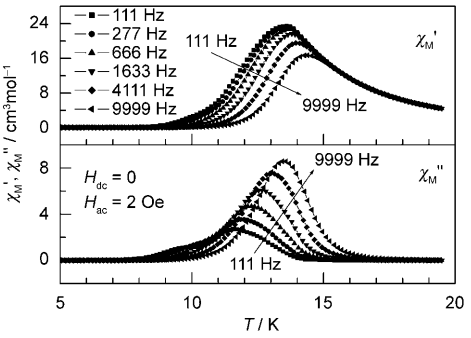

Figure 4. Temperature dependence of AC susceptibilities of a polycrystalline sample of **2** under a 0 Oe DC field within the frequency range 111–9999 Hz.

At 1.8 K, the isothermal magnetizations (Figure 5, top) displayed a hysteresis loop with a quite large coercive field, H_C^{powder}, of 17.5 kOe and a saturated magnetization of 3.17 Nβ (at 70 kOe), hence the material was a hard magnet at this temperature. A few Co chain compounds have previously been reported to show such large coercivity.[4,13b] On warming, the hysteresis loop drastically diminished and almost disappeared at 7 K, indicating that above this temperature the material was transformed from a hard to a very soft magnet. The sharp increase in the ZFC above 7 K confirmed this behavior. This behavior is very similar to that of

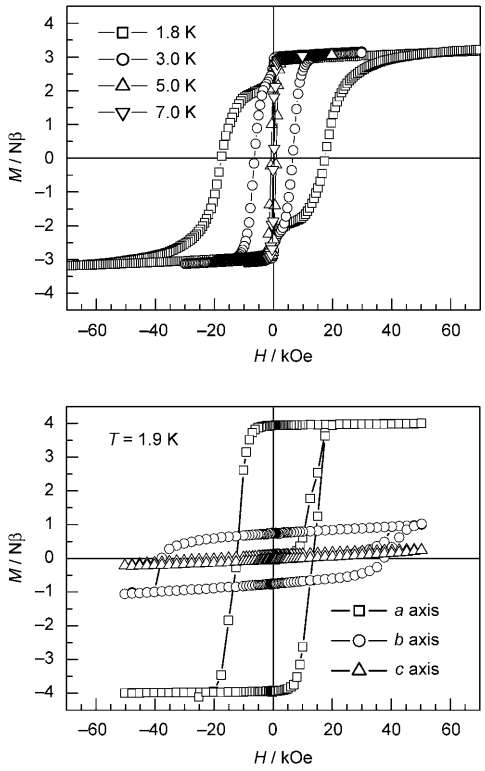

Figure 5. Isothermal magnetization plots for **2**: Top) for a polycrystalline sample; bottom) for a single crystal with crystallographic *a*, *b*, and *c* axes parallel to the external field.

the very recently reported chain-like compound [Co(hfac)$_2$BPNN] (hfac = 1,1,1,5,5,5-hexafluoro-2,4-pentanedione; BPNN = *p*-butoxyphenyl-4,4,5,5-tetramethyl-imidazolin-1-oxyl-3-oxide).[13b]

To estimate the magnetic couplings within the material, the high-temperature susceptibility data (above 50 K) were simulated by Fisher's 1D Heisenberg chain model[18] ($S=3/2$, $H=-2JS_iS_j$, zJ' being the intrachain interaction), as used for other Co chain compounds,[6a] in conjunction with consideration of the interchain interaction (zJ') in terms of mean field theory.[1f,21] This gave $J=10.0(4)$ cm^{-1}, $zJ'=0.3(1)$ cm^{-1}, $g=2.71(2)$, and $R=3.2\times10^{-4}$ (R defined as before). The intrachain coupling J was comparable to that found in the EO-azido-bridged SCM formed by the [Co(bt)$(N_3)_2$] chain ($J=6.2$ cm^{-1}, $H=-2JS_iS_j$) and the dimer of [Co(L)$(N_3)_2$] ($J=7.2$ cm^{-1}, $H=-2JS_iS_j$) (L = 2,9-dimethyl-1,10-phenanthroline),[6a] and the positive interchain coupling (zJ') indicated the global FO coupling within the compound. The one-dimensional nature of the magnetism of **2** was proved by the fact that J was about 30 times higher than zJ', and this verified the success of our synthetic approach to 1D systems by using long spacers.

Since large-sized single crystals of **2** were available, it was possible to perform magnetic studies on these. As **2** forms orthorhombic crystals, the three crystal axes are the magnetically principal ones.[22] Hereafter, the symbol A^i represents the magnetic variable A along the i axis. Rotation measurements (Figure 6) revealed strong magnetic anisotropy, with

 © 2009 Wiley-VCH Verlag GmbH & Co. KGaA, Weinheim

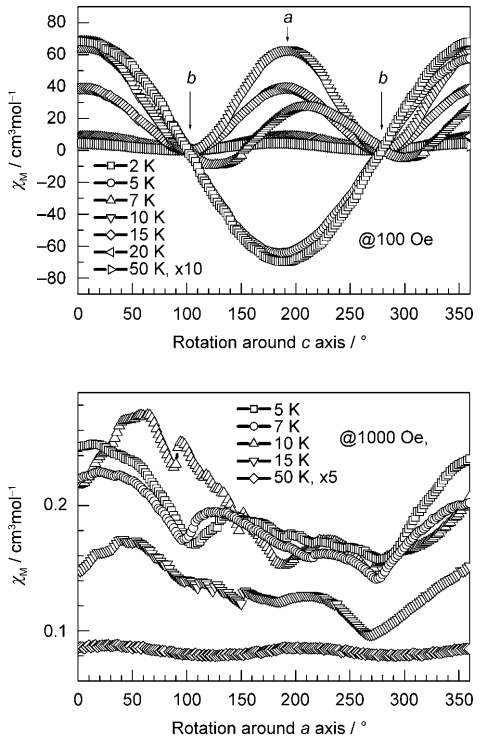

Figure 6. Rotation measurements about the top) *c* axis and about the bottom) *a* axis for single crystals.

the *a* axis being the easy one and the *b* and *c* axes being the hard ones. In rotation measurements about the *c* axis at different temperatures (Figure 6, top), the crystal behaved as a small permanent magnet with its magnetization direction along the *a* axis at 2 and 5 K, while at 7 K the rotation data displayed relaxation behavior. Above 7 K, the sample exhibited a sinusoidal rotation curve of high anisotropy, with maxima in the *a* direction and minima in the *b* direction. Even at 50 K, the ratio of $\chi_M{}^a$ to $\chi_M{}^b$ was 22. The rotation data about the *a* axis (Figure 6, bottom), however, displayed only small anisotropy and some irregularity. In the ZFC/FC plots (Figure 7) under a 10 Oe field, $\chi_M{}^a$, $\chi_M{}^b$, and $\chi_M{}^c$ are seen to be similar in shape, but $\chi_M{}^a$ is about 100 times larger than $\chi_M{}^b$ and $\chi_M{}^c$. This confirmed that the system was of a strongly magnetically anisotropic Ising type,[23] with the *a* axis as the easy axis and the spin orientation direction. A kink at around 10 K was observed in the three FC plots (most distinct for the $\chi_M{}^a$ data; less significant for the $\chi_M{}^b$, $\chi_M{}^c$, and $\chi_M{}^{powder}$ data) and in a plot of $d\chi_M{}^a/dT$ for the FC data (Figure S3 in the Supporting Information). Beside the large negative peak at 13.8 K, a small but obvious peak was observed at 9.9 K. This was suggestive of a second magnetic transition in the low-temperature region, as had also been indicated by the previous AC measurements at low frequencies (Figure 4). A primary specific heat (C_P) measurement on one single crystal (Figure S4 in the Supporting Information) also confirmed the LRO of FO at a T_C of 13.6 K through a small kink in the plot. Above T_C, a broad hump was seen in the magnetic specific heat (C_M), probably reflecting the short-range order of the Ising-like chain,[1c] while below T_C the specific heat decreased smoothly and continuously. The magnetic anisotropy persisted over the whole temperature region, although it was not so significant in the high-temperature region (Figure S5 in the Supporting Information). Under a 5 kOe field, the $\chi_M T^a$ value at 300 K (6.7 $cm^3 mol^{-1} K$) was more than twice as large as $\chi_M T^b$ or $\chi_M T^c$ (2.4 and 2.6 $cm^3 mol^{-1} K$, respectively). On cooling, $\chi_M T^a$ continuously increased. Below 50 K, it increased sharply, reaching a maximum of 69 $cm^3 mol^{-1} K$ at 19 K before decreasing once more on further cooling. On the other hand, both $\chi_M T^b$ and $\chi_M T^c$ first decreased, reaching minima of 1.6 $cm^3 mol^{-1} K$ at 50 K and 0.6 $cm^3 mol^{-1} K$ at 18 K, respectively, before increasing to maxima of 10.7 $cm^3 mol^{-1} K$ at 14 K and 0.9 $cm^3 mol^{-1} K$ at 13 K, respectively, and finally decreasing again on further cooling. It is clear that the magnetic behavior parallel to the *a* axis dominates the magnetism of the material, and the initial decreases of $\chi_M T^b$ and $\chi_M T^c$ are presumably due to the effect of spin-orbital coupling of the Co^{2+} ion, resulting in an effective $S=1/2$ at low temperature as opposed to $S=3/2$ at high temperature.[1,20]

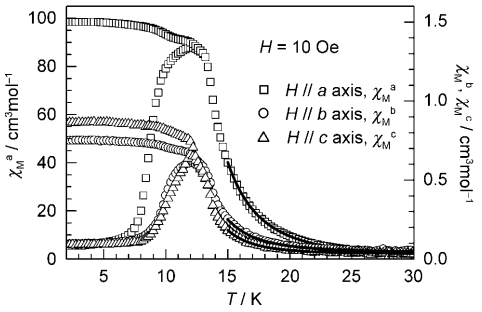

Figure 7. ZFC/FC plots under a 10 Oe field for a single crystal with the applied field parallel to the crystallographic *a*, *b*, and *c* axes, respectively. The thick black lines are the best fits obtained by using an Ising chain model (see text).

The FC susceptibility data under a 10 Oe field in the range 15–30 K (Figure 7) were simulated by using an $S=1/2$ Ising chain model.[1e,f,23a] For the $\chi_M{}^a$ data, the expression for the parallel susceptibility[1e,f,23a] was used, and the fitting procedure resulted in $J=48.2(1)$ cm^{-1} and $g^a=7.95(1)$ with $R=2.5\times10^{-5}$ (R defined as before). $\chi_M{}^b$ and $\chi_M{}^c$, on the other hand, were fitted using the expression for a combination ($\chi_{M\parallel}\cos^2\alpha+\chi_{M\perp}\sin^2\alpha$) of the parallel ($\chi_{M\parallel}$) and perpendicular ($\chi_{M\perp}$) susceptibilities by rotation of the susceptibility tensor over the angle α between the magnetic field and the preferred axis, taking into consideration the mismatch between the magnetic field and the crystal orientation.[24] The best fitting produced $J=52(1)$ cm^{-1}, $g^b=5.0(1)$, and $\alpha=3.5(2)°$ with $R=6.4\times10^{-4}$ for the $\chi_M{}^b$ data, and $J=61(2)$ cm^{-1}, $g^c=4.9(1)$, and $\alpha=1.9(2)°$ with $R=2.0\times10^{-3}$ for the $\chi_M{}^c$ data. The result of $g^a>g^b$ and g^c further corroborated the Ising nature of this compound.[23b,24]

Very large anisotropy was also observed for the isothermal magnetizations of the single crystal (Figure 5, bottom).

 © 2009 Wiley-VCH Verlag GmbH & Co. KGaA, Weinheim

At 1.9 K, the magnetization M^a maintained low values below 10 kOe, then quickly reached the saturation $M_S{}^a$ of 4.0 Nβ. The coercive field $H_C{}^a$ of the hysteresis loop was 13.6 kOe. When the external field was applied along the *b* and *c* axes, the hysteresis loops were much more flat, but $H_C{}^b$ and $H_C{}^c$ were 37.5 kOe and 13.2 kOe, respectively. The large $H_C{}^b$ of 37.5 kOe can be expected to contribute to the quite large $H_C{}^{powder}$ of 17.5 kOe, which is comparable to the values for very hard magnets such as $SmCo_5$ or $Nd_2Fe_{14}B$ (44 and 19 kOe, respectively, at room temperature).[25] For molecular-based materials, such a value is still quite unusual.[4,13b,26] Only a few molecular-based materials have hitherto been found to display such large H_C values, for example, 27.8 kOe observed for [MnTBrPP][TCNE] (FI) at 2 K,[26a] 17.8 kOe for $[Fe(dca)_2]$ (dca = dicyanamide) (FO) at 2 K,[26b] and 21.7 kOe for the Co chain compound $[Co_3(bime)_2(\mu_3\text{-}OH)_2(HO\text{-}BDC)_2]_n$ (bime = 1,2-bis(imidazol-1-yl)ethane; HO-BDC = 5-hydroxy-isophthalate) (FI) at 1.8 K.[4] The largest H_C value of 52 kOe at 6 K has recently been reported for [Co(hfac)$_2$BPNN] (FI),[13b] which is considered to result from the underlying Glauber dynamics or the difficulty in reversal of the magnetization within the $[Co(hfac)_2BPNN]_n$ chain below the freezing temperature of 10 K in such quasi-1D systems.[13a,b]

The observed strong anisotropy in **2** stems from the magnetic anisotropy of Co^{2+} due to the unquenched orbital contribution.[1a,c] It is well known that a Co^{2+} ion in an octahedral field has a $^4T_{1g}$ ground state. Under spin-orbit coupling, this splits into a set of three levels with a doubly-degenerate level, leading to an effective $S=1/2$ ground state with a large *g* value in the low-temperature region.[1a,c] The tetragonal distortion generally results in a singlet ground state of $^4T_{2g}$ and a doublet excited state of ^4E_g, which also affects the anisotropy of the Co^{2+} ions.[1a] For a Co^{2+} ion in elongated tetrahedral distortion, it usually shows XY nature.[27] However, in a compressed tetrahedral distortion, a Co^{2+} ion shows Ising anisotropy with its easy axis along the axial direction,[5a] as is the case for **2** here. Another origin of anisotropy is the alignment of the individual easy axes. In **2**, the easy axis of the Co^{2+} ion is along the O-Co-O direction. The straight chains and their parallel packing in the structure make all O-Co-O axes completely parallel, thus further enhancing the anisotropy of the material.[13a] This is quite different from the cases of the first SCM compounds based on Co^{2+} and radicals[3a] and $[Co(bt)(N_3)_2]$,[6a] in which the non-collinearity of individual easy axes reduced the observed anisotropy of the systems.[13a]

Finally, AC susceptibility studies on the polycrystalline sample revealed more features of the magnetism of **2** in the low-temperature range (Figures 4 and 8; Figures S6, S7, and S8 in the Supporting Information). In zero DC field, both the χ_M' and χ_M'' signals showed two frequency-dependent peaks. The high-temperature peak in the region 11–15 K was high in signal but weak in frequency-dependence, with a $\varphi=(\Delta T_P/T_P)/\Delta(\log f)$ of 0.09 (T_P is the peak temperature of χ'' and f the AC frequency), this being typical for a spin glass.[28] The low-temperature peak in the region 5–11 K was much lower in signal but showed a strong frequency dependence. The φ value was 0.17, characterizing a superparamagnetic behavior.[2–6] This magnetic relaxation was fitted by the Arrhenius law, $\tau=\tau_0\exp(E_a/k_BT)$, which resulted in $\tau_0=2.5\times10^{-9}$ s and $E_a/k_B=56$ K (Figure S6 in the Supporting Information) using the low-frequency data (Figure 8). These results are comparable to data for other homometallic Co chains,[4,6a] but E_a/k_B is much lower than those reported for Co-radical chains.[3a,13b] The result puts the dynamic process of τ on a timescale of hours at 1.8 K, which shifts to a μs timescale above 7 K. Another observation was that the high-temperature peak could be somewhat suppressed by the applied DC field (Figure S7 in the Supporting Information), similar to earlier observations for several homometallic Co chains.[4,6a,13c] The increased DC field further weakened the AC responses of the material and the AC responses above 2.5 kOe (for out-of-phase) and 3.0 kOe (for in-phase) were lowered to noise level (Figure S8 in the Supporting Information). Due to the fact that the Co azido chains are weakly coupled in **2**, the magnetic relaxation or SCM-like behavior in the low-temperature region may stem from either: 1) the finite size effect of the FO chain as a result of defects,[29] or 2) the intrinsic Glauber dynamics within such a strongly anisotropic chain.[13a] Clearly, this merits further investigation.

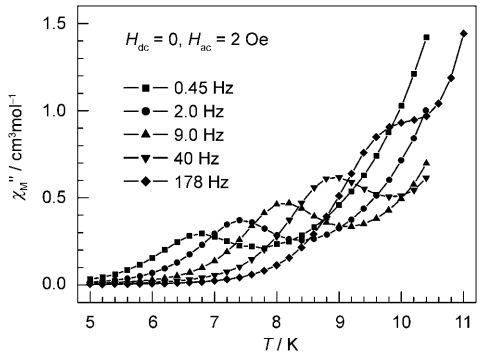

Figure 8. Second, small peak in the out-of-phase AC susceptibilities for a polycrystalline sample of **2** in the low-frequency range under a zero DC field.

Conclusion

In summary, we have successfully obtained two isostructural double-EO-azido-bridged magnetic chain compounds by using the long spacer bpeado. The metal-azido chains are supported by H-bonding interactions with lattice bpeado, and are thus embedded in a 3D threefold interpenetrated H-bonded framework. The chains are quite well separated within the structures. Investigation of the magnetic properties has revealed that **1** comprises isotropic Heisenberg chains with unusual AF coupling between the double-EO-azido-bridged Mn^{2+} ions. However, the anisotropic Co^{2+} ions in **2** resulted in a strong Ising-type FO chain. Large coercivity up to 37.5 kOe along the crystallographic *b* axis,

 © 2009 Wiley-VCH Verlag GmbH & Co. KGaA, Weinheim

multi-magnetic transitions, and SCM-like magnetic relaxation have been observed for **2**. This work has provided an opportunity for exploring the influence of magnetic anisotropy of the spin carriers and their coupling on the magnetic behavior of 1D systems, control of the synthesis of SCMs, and the magnetism of weakly coupled SCMs.

Experimental Section

Synthesis: All starting materials were reagent grade from commercial sources and were used without further purification. The ligand bpeado was prepared from 1,2-bis(4-pyridyl)ethane according to the literature method.[30]

CAUTION! Azide salts are potentially explosive; such compounds should be synthesized and used in small quantities, and treated with the utmost care at all times.

$[Mn(N_3)_2(H_2O)_2]\cdot$(bpeado) (1): $MnCl_2\cdot 4H_2O$ (0.50 mmol, 100 mg) and bpeado (0.50 mmol, 108 mg) were dissolved in water (10 mL). NaN_3 (1.0 mmol, 65 mg) was then added under continuous stirring. A light-yellow precipitate formed. The system was heated to give a clear yellow solution, which was then filtered. The water was allowed to slowly evaporate from the filtrate at room temperature. Light-yellow single crystals were harvested after one day, which were washed with water and dried in air (80%). IR (N_3^-): $\tilde{\nu}=2078$ (s), 2042 cm^{-1} (s); elemental analysis calcd (%) for $C_{12}H_{16}MnN_8O_4$: C 36.84, H 4.12, N 28.64; found: C 37.00, H 4.05, N 29.12.

$[Co(N_3)_2(H_2O)_2]\cdot$(bpeado) (2): A similar preparation route using $CoCl_2\cdot 6H_2O$ gave crystals of **2** in 85% yield. IR (N_3^-): $\tilde{\nu}=2070$ (s), 2035 cm^{-1} (s); elemental analysis calcd (%) for $C_{12}H_{16}CoN_8O_4$: C 36.48, H 4.08, N 28.35; found: C 36.41, H 4.01, N 28.84. Large single crystals were obtained by carefully controlled crystallization over a period of two weeks. The crystals proved to be stable and remained unchanged when stored in the ambient environment for more than two years.

X-ray crystallography and physical measurements: Crystallographic data for **1** and **2** were collected at 293 K on a Nonius KappaCCD diffractometer using graphite-monochromated $Mo_{K\alpha}$ radiation ($\lambda=0.71073$ Å).[31] Empirical absorption corrections were applied using the Sortav program.[32] The structures were solved by direct methods and refined by full-matrix least-squares on F^2 using the SHELX program[33] with anisotropic thermal parameters for all non-hydrogen atoms. Hydrogen atoms of water molecules were located by difference Fourier maps and were refined with constraints for the ideal geometry of a water molecule, with an O-H distance of 0.96 Å, an H-O-H angle of 105°, and the same isotropic thermal factor. Other hydrogen atoms were placed in calculated positions. Crystallographic data for **1** and **2** are listed in Table 1, and selected bond lengths and angles are given in Table 2. CCDC 677366 (**1**) and 677367 (**2**) contain the supplementary crystallographic data for this paper. These data can be obtained free of charge from The Cambridge Crystallographic Data Centre via www.ccdc.cam.ac.uk/data_request/cif. A CIF file of **1** and **2** can also be found in the Supporting Information.

PXRD data for the two compounds were collected in the range $5 < 2\theta < 60°$ at room temperature on bulk samples with a Rigaku Dmax 2000 diffractometer in flat-plate geometry using $Cu_{K\alpha}$ radiation. The experimental PXRD patterns were in good agreement with those calculated from the single-crystal structures (Figure S1 in the Supporting Information), confirming the phase purity of the bulk samples.

Elemental analyses of carbon, hydrogen, and nitrogen were performed on an Elementar Vario El analyzer. IR spectra were recorded from pure samples on a Nicolet Magna-IR 750 spectrometer equipped with a Nic-Plan microscope.

Magnetic measurements and specific heat capacity measurements on polycrystalline samples and single crystals of mass about 1.0 mg were carried out on a Quantum Design MPMS XL-5 SQUID System and an Oxford Maglab^{2000} System. In magnetic measurements on single crystals, the orientation accuracy of the axes was estimated as several degrees. Identification of the crystallographic axes with respect to the morphology of the single crystal was performed on the Nonius KappaCCD diffractometer. The crystals had elongated plate shapes, with the *ac* plane within the plate, the *c* axis along the long axis of the sample, and the *b* axis perpendicular to the plate plane. All experimental magnetic data, except for the rotation data, were corrected for the diamagnetism of the sample holders and of the constituent atoms (Pascal's tables).[34]

Acknowledgements

This work was supported by the National Natural Science Foundation of China (Grants 20221101, 20490210, 20503001, and 20571005), the National Basic Research Program of China (Grant 2006CB601102), and the Research Fund for the Doctoral Program of Higher Education (Grant 20050001002).

[1] a) O. Kahn, *Molecular Magnetism*, Wiley-VCH, Weinheim, **1993**; b) J. S. Miller, M. Drillon, *Magnetism: Molecules to Materials I*, Wiley-VCH, Weinheim, **2001**; c) R. L. Carlin, *Magnetic Property of Transition Metal Compounds*, Springer, New York, **1977**; d) L. J. de Jongh in *Magneto-Structural Correlations in Exchange Coupled Systems* (Eds.: R. D. Willett, D. Gatteschi, O. Kahn), D. Reidel Publishing Company, Dordrecht, **1985**, pp. 1–35; e) J. S. Miller, *Extended Linear Chain Compounds, Vol. 3*, Plenum Press, New York, **1983**, pp. 43–191; f) R. L. Carlin, *Magnetochemistry*, Springer, Heidelberg, **1986**, Chapter 7.

[2] a) C. Coulon, H. Miyasaka, R. Clérac, *Struct. Bonding (Berlin)* **2006**, *122*, 163 and references therein; b) L. Bogani, A. Vindigni, R. Sessolia, D. Gatteschia, *J. Mater. Chem.* **2008**, *18*, 4750 and references therein.

[3] a) A. Caneschi, D. Gatteschi, N. Lalioti, C. Sangregorio, R. Sessoli, G. Venturi, A. Vindigni, A. Rettori, M. G. Pini, M. A. Novak, *Angew. Chem.* **2001**, *113*, 1810; *Angew. Chem. Int. Ed.* **2001**, *40*, 1760; b) R. Clérac, H. Miyasaka, M. Yamashita, C. Coulon, *J. Am. Chem. Soc.* **2002**, *124*, 12837; c) Z. M. Sun, A. V. Prosvirin, H. H. Zhao, J. G. Mao, K. R. Dunbar, *J. App. Phys.* **2005**, *97*, 10B305; d) L. Bogani, C. Sangregorio, R. Sessoli, D. Gatteschi, *Angew. Chem.* **2005**, *117*, 5967; *Angew. Chem. Int. Ed.* **2005**, *44*, 5817; e) H. Miyasaka, T. Madanbashi, K. Sugimoto, Y. Nakazawa, W. Wernsdorfer, K. Sugiura, M. Yamashita, C. Coulon, R. Clérac, *Chem. Eur. J.* **2006**, *12*, 7028; f) K. Bernot, L. Bogani, A. Caneschi, C. Sangregorio, R. Sessoli, D. Gatteschi, *J. Am. Chem. Soc.* **2006**, *128*, 7947.

[4] X. J. Li, X. Y. Wang, S. Gao, R. Cao, *Inorg. Chem.* **2006**, *45*, 1508.

[5] a) R. Lescouëzec, J. Vaissermann, C. Ruiz-Perez, F. Lloret, R. Carasco, M. Julve, M. Verdaguer, Y. Dromzee, D. Gatteschi, W. Wernsdorfer, *Angew. Chem.* **2003**, *115*, 1521; *Angew. Chem. Int. Ed.* **2003**, *42*, 1483; b) S. Wang, J. L. Zuo, S. Gao, Y. Song, H. C. Zhou, Y. Z. Zhang, X. Z. You, *J. Am. Chem. Soc.* **2004**, *126*, 8900; c) L. M. Toma, R. Lescouëzec, J. Pasan, C. Ruiz-Perez, J. Vaissermann, J. Cano, R. Carrasco, W. Wernsdorfer, F. Lloret, M. Julve, *J. Am. Chem. Soc.* **2006**, *128*, 4842.

[6] a) T. F. Liu, D. Fu, S. Gao, Y. Z. Zhang, H. L. Sun, G. Su, Y. J. Liu, *J. Am. Chem. Soc.* **2003**, *125*, 13976; b) X. T. Liu, X. Y. Wang, W. X. Zhang, P. Cui, S. Gao, *Adv. Mater.* **2006**, *18*, 2852; c) H. B. Xu, B. W. Wang, F. Pan, Z. M. Wang, S. Gao, *Angew. Chem.* **2007**, *119*, 7532; *Angew. Chem. Int. Ed.* **2007**, *46*, 7388.

[7] a) E. Pardo, R. Ruiz-Garcia, F. Lloret, J. Faus, M. Julve, Y. Journaux, F. Delgado, C. Ruiz-Perez, *Adv. Mater.* **2004**, *16*, 1597; b) E. Pardo, R. Ruiz-Garcia, F. Lloret, J. Faus, M. Julve, Y. Journaux, M. A. Novak, F. S. Delgado, C. Ruiz-Perez, *Chem. Eur. J.* **2007**, *13*, 2054.

[8] a) Y. Z. Zheng, M. L. Tong, W. X. Zhang, X. M. Chen, *Angew. Chem.* **2006**, *118*, 6458; *Angew. Chem. Int. Ed.* **2006**, *45*, 6310; b) Y. L. Bai, J. Tao, W. Wolfgang, O. Sato, R. B. Huang, L. S. Zheng, *J. Am. Chem. Soc.* **2006**, *128*, 16428.

 © 2009 Wiley-VCH Verlag GmbH & Co. KGaA, Weinheim

[9] a) M. A. M. Abu-Youssef, A. Escuer, D. Gatteschi, M. A. S. Goher, F. A. Mautner, R. Vicente, *Inorg. Chem.* **1999**, *38*, 5716; b) S. Q. Bai, E. Q. Gao, Z. He, C. J. Fang, Y. F. Yue, C. H. Yan, *Eur. J. Inorg. Chem.* **2006**, 407; c) M. A. M. Abu-Youssef, A. Escuer, V. Langer, *Eur. J. Inorg. Chem.* **2006**, 3177; d) X. Y. Wang, Z. M. Wang, S. Gao, *Chem. Commun.* **2008**, 281.
[10] a) M. A. M. Abu-Youssef, A. Escuer, M. A. S. Goher, F. A. Mautner, G. Reiss, R. Vicente, *Angew. Chem.* **2000**, *112*, 1681; *Angew. Chem. Int. Ed.* **2000**, *39*, 1624; b) M. A. M. Abu-Youssef, M. Drilion, A. Escuer, M. A. S. Goher, F. A. Mautner, R. Vicente, *Inorg. Chem.* **2000**, *39*, 5022; c) J. Cano, Y. Journaux, M. A. S. Goher, M. A. M. Abu-Youssef, F. A. Mautner, G. J. Reiss, A. Escuer, R. Vicente, *New J. Chem.* **2005**, *29*, 306.
[11] T. Liu, Y. Zhang, Z. Wang, S. Gao, *Inorg. Chem.* **2006**, *45*, 2782.
[12] a) H. L. Sun, S. Gao, B. Q. Ma, S. R. Batten, *CrystEngComm* **2004**, *6*, 579; b) H. L. Sun, B. Q. Ma, S. Gao, S. R. Batten, *Cryst. Growth Des.* **2005**, *5*, 1331.
[13] a) R. Sessoli, *Angew. Chem.* **2008**, *120*, 5590; *Angew. Chem. Int. Ed.* **2008**, *47*, 5508; b) N. Ishii, Y. Okamura, S. Chiba, T. Nogami, T. Ishida, *J. Am. Chem. Soc.* **2008**, *130*, 24; c) Z. He, Z. M. Wang, S. Gao, C. H. Yan, *Inorg. Chem.* **2006**, *45*, 6694.
[14] a) L. Lecren, W. Wernsdorfer, Y. G. Li, A. Vindigni, H. Miyasaka, R. Clérac, *J. Am. Chem. Soc.* **2007**, *129*, 5045; b) H. Miyasaka, M. Yamashita, *Dalton Trans.* **2007**, 399; c) W. Wernsdorfer, N. Aliaga-Alcalde, D. N. Hendrickson, G. Christou, *Nature* **2002**, *416*, 406.
[15] G. R. Desiraju, T. Steiner, *The Weak Hydrogen Bond In Structural Chemistry and Biology*, Oxford University Press, New York, **1999**.
[16] C. Janiak, *J. Chem. Soc. Dalton Trans.* **2000**, 3885.
[17] *Theory and Application of Molecular Paramagnetism* (Eds.: E. A. Boudreaux, J. N. Mulay), Wiley, New York, **1976**.
[18] M. E. Fisher, *Am. J. Phys.* **1964**, *32*, 343.
[19] E. Ruiz, J. Cano, S. Alvarez, P. Alemany, *J. Am. Chem. Soc.* **1998**, *120*, 11122.
[20] a) K. Kambe, S. Koide, Y. Usui, *Prog. Theor. Phys.* **1952**, *7*, 15; b) H. L. Sun, S. Gao, B. Q. Ma, G. Su, *Inorg. Chem.* **2003**, *42*, 5399.
[21] a) B. E. Myers, L. Berger, S. Friedberg, *J. Appl. Phys.* **1969**, *40*, 1149; b) C. J. O'Connor, *Prog. Inorg. Chem.* **1982**, *29*, 203.
[22] M. Gerloch, *Magnetism and Ligand-Field Analysis*, Cambridge University Press, London, **1983**, pp. 147–152.
[23] a) M. E. Fisher, *J. Math. Phys.* **1963**, *4*, 124; b) A. Caneschi, D. Gatteschi, N. Lalioti, R. Sessoli, L. Sorace, V. Tangoulis, A. Vindigni, *Chem. Eur. J.* **2002**, *8*, 286.
[24] H. A. Groenendijk, A. J. V. Duyneveldt, *Physica* **1982**, *115B*, 41.
[25] J. Fidler, T. Schrefl, S. Hoefinger, M. Hajduga, *J. Phys. Condens. Matter* **2004**, *16*, S455.
[26] a) D. K. Rittenberg, K. Sugiura, Y. Sakata, S. Mikami, A. J. Epstein, J. S. Miller, *Adv. Mater.* **2000**, *12*, 126; b) M. Kurmoo, C. J. Kepert, *New J. Chem.* **1998**, *22*, 1515.
[27] A. Bencini, C. Benelli, D. Gatteschi, C. Zanchini, *Inorg. Chem.* **1980**, *19*, 1301.
[28] J. A. Mydosh, *Spin Glass: An Experimental Introduction*, Taylor Francis, London, **1993**.
[29] L. Bogani, A. Caneschi, M. Fedi, D. Gatteschi, M. Massi, M. A. Novak, M. G. Pini, A. Rettori, R. Sessoli, A. Vindigni, *Phys. Rev. Lett.* **2004**, *92*, 207204.
[30] P. G. Simpson, A. Vinciguerra, J. V. Quagliano, *Inorg. Chem.* **1963**, *2*, 282.
[31] a) "*Collect*" data collection software, Nonius BV, Delft, **1998**; b) "HKL2000" and "maXus" softwares, University of Glasgow, Nonius BV, Delft, and MacScience Co. Ltd., Yokohama, **2000**.
[32] a) R. H. Blessing, *Acta Crystallogr. Sect. A* **1995**, *51*, 33; b) R. H. Blessing, *J. Appl. Crystallogr.* **1997**, *30*, 421.
[33] a) G. M. Sheldrick, *SHELXTL* Version 5.1. Bruker Analytical X-ray Instruments Inc., Madison, Wisconsin, **1998**; b) G. M. Sheldrick, *SHELX-97*, PC Version, University of Göttingen, **1997**.
[34] E. A. Boudreaux, J. N. Mulay, *Theory and Application of Molecular Diamagnetism*, Wiley, New York, **1976**.

Received: August 14, 2008
Published online: January 2, 2009

 © 2009 Wiley-VCH Verlag GmbH & Co. KGaA, Weinheim